Behavior of photoconductivity transients due to multiple trapping by a Gaussian distribution of localized states

Serge Grabtchak* and Michael Cocivera
Guelph-Waterloo Centre for Graduate Work in Chemistry, University of Guelph, Guelph, Ontario N1G 2W1, Canada
(Received 19 April 1999)

The decay of excess carriers in semiconductors was analyzed under conditions of multiple trapping by a Gaussian distribution of subband gap states and recombination. Numerical solutions to the rate equations involving multiple trapping in subband gap states and recombination indicate that a power-law decay is observed only under limited conditions. The concept of an optimally filled energy level for which a ratio of the trapping time to the release time has a minimum is introduced for the Gaussian distribution. We showed that the position of the Fermi level may limit the portion of the distribution that can be effective in the decay. The results provide an explanation for the nonlinear temperature dependence of the exponential term α_1 that is sometimes observed experimentally. [S0163-1829(99)11039-7]

I. INTRODUCTION

Polycrystalline-thin film and amorphous semiconductors have applications in a variety of devices such as arrays of light sensors, thin-film transistors, photovoltaic cells, flat panel displays, etc. Understanding the fundamental properties of these materials is important for any applications. Due to complicated trapping/retrapping dynamics, localized state distributions often present in semiconductor materials may affect these properties. Fourier[2] and Laplace[3] transformations of transient photoconductivity and transient photocurrent kinetics[1–3] have shown that very structured distributions can result from this analysis. Such distributions may include any combination of some elementary density of states (DOS), i.e., exponential, rectangular, linear, and peaked Gaussian. Another method, photoinduced midgap absorption (PA),[4–6] uses a pump beam to produce excess carriers that populate localized states in a band gap. Densities of these localized carriers are inferred by absorption of a subsequent probe beam. A relatively new method, (advanced method of transient microwave photoconductivity) simultaneously provides data corresponding to both of these methods by measuring the effect of free and localized carriers on the imaginary and real parts of the complex dielectric constant.[7] It should be pointed out that the excess carriers measured by these techniques are ultimately removed by recombination. As a result the phenomenon differs from time of flight in which excess carriers are removed by transit from one contact to the other.

Because the density of states (DOS) distribution is the link between the multiple trapping model and the experimental data, it is important to understand how the type of distribution affects the decay kinetics so that the type of distribution may be inferred less ambiguously from kinetic data. Simulated transients based on certain DOS distributions have been compared under limited conditions.[8,9] More recently, we have used numerical solution of rate equations involving multiple trapping to establish the characteristic effects of rectangular/linear[10] and exponential[11,12] distributions on the transient decays of excess free and localized carriers. To round out these studies, the present paper reports the characteristics of the peaked Gaussian distribution, which frequently is found in disordered systems.[13,14] In contrast to exponential, rectangular and linear DOS, this distribution has a region where the density of states increases with increasing energy. As a result, this DOS can cause more complex decay kinetics, and this paper highlights the more important features for photocurrent and photoconductivity. Manifestations of the Gaussian DOS in photoabsorption and photodielectric effect measurements are currently under study.

Knowledge of the behavior of the Gaussian distribution is essential to compare the effects of various distributions on non-equilibrium charge carrier dynamics. However, there may be cases in which experimentally observed dependency will deviate from those expected for the classical Gaussian distribution. The extent of this deviation will depend on the position of the Fermi level relative to the distribution. In this situation, the distribution is distorted from a Gaussian form. The present paper considers the effects of the pure Gaussian distribution first. Then, the more complicated situation involving the position of the Fermi level is considered to illustrate that it provides a possible explanation to the unusual temperature dependence of the power-law decays reported in number of papers.

II. DETAILS OF THE NUMERICAL SOLUTION

The continuous Gaussian DOS function was replaced by a set of m discrete levels separated by spacing Δ so that the energy of ith level is $\delta E_i = -E_l - \Delta i$, where E_l is a variable offset energy. The concentration of corresponding traps is $N_i = g_i \Delta$, where $g_i = g_0 \exp\{-[(\delta E_i - E_0)/kT_0]^2\}$ and E_0 corresponds to a peak energy position, T_0 is a characteristic temperature describing the width of the distribution. The release probability r_i and the capture probability $\omega_i(t)$ including a provision for trap saturation are

$$\omega_i(t) = [N_i - \Delta n_i(t)] S v$$
$$r_i = v_0 \exp(\delta E_i / kT), \tag{1}$$

in which $S=10^{-15}\,\mathrm{cm}^2$ is the capture cross section, v is the thermal velocity and v_0 is the attempt-to-escape frequency ($10^{12}\,\mathrm{s}^{-1}$). All other parameters used in the numerical solutions are given below. The multiple trapping rate equations are

$$\frac{d\Delta n(t)}{dt}=\sum_{i=1}^{m} r_i\Delta n_i(t)-\Delta n(t)\sum_{i=1}^{m}\omega_i(t)-\Delta n(t)/\tau_r$$
$$\frac{d\Delta n_i(t)}{dt}=\Delta n(t)\omega(t)_i-\Delta n_i(t)r_i \tag{2}$$

in which $\Delta n(t)$ is the concentration of excess free electrons, $\Delta n_i(t)$ is the concentration of excess electrons trapped in the ith level and τ_r is a time constant for monomolecular recombination. Because Eq. (2) includes nonlinear effects due to trap filling, they are an improvement over the linear system used earlier.[10]

III. RESULTS OF THE NUMERICAL SOLUTIONS

1. Behavior of $\Delta n(t)$—the effect of g_0.

Frequently photoconductivity transients exhibit a power-law dependence ($t^{(\alpha-1)}$ and $t^{(-\alpha-1)}$). To determine conditions under which the Gaussian DOS provides a power law behavior we employ an approach used for other distributions.[10,12] The density of states g_0 was varied from $10^{14}\,\mathrm{cm}^{-3}\,\mathrm{eV}^{-1}$ to $10^{21}\,\mathrm{cm}^{-3}\,\mathrm{eV}^{-1}$ keeping all other parameters of the numerical calculation constant. In addition for each g_0, the initial excess electron concentration Δn_0 was varied from 10^{22} to $10^{11}\,\mathrm{cm}^{-3}$ to explore the effect of trap saturation. Other parameters were: $m=26$, $T_0=800\,\mathrm{K}$, $T=300\,\mathrm{K}$, $\Delta=0.025\,\mathrm{eV}$, $\tau_r=10^{-8}\,\mathrm{s}$, $E_0=0.5\,\mathrm{eV}$, $E_1=0.3\,\mathrm{eV}$. For each distribution, comparison of the recombination time τ_r with the average trapping time, $\tau_{\downarrow av}=1/(Sv\Sigma_{i=1}^{n}N_i)$, indicated that the behavior of $\Delta n(t)$ was governed by three empirically found distinct conditions: (i) $\tau_{\downarrow av}\cong 0.1\tau_r$, (ii) $\tau_{\downarrow av}<0.1\tau_r$, (iii) $\tau_{\downarrow av}>0.1\tau_r$. In general, transition from one power law ($t^{(\alpha-1)}$) to the other ($t^{(-\alpha-1)}$) occurred only for condition (i) (Fig. 1). As a result the absence of power-law behavior in $\Delta n(t)$ does not preclude the Gaussian DOS.

Condition (i) is satisfied only for $g_0=10^{18}\,\mathrm{cm}^{-3}\,\mathrm{eV}^{-1}$, and the behavior of $\Delta n(t)$ is given in Fig. 1. The seven curves correspond to various values of Δn_0 ($10^{22}-10^{11}\,\mathrm{cm}^{-3}$). The total electron trap concentration is $N_\Sigma=0.12\times10^{18}\,\mathrm{cm}^{-3}$, which corresponds to an average trapping time $\tau_{\downarrow av}=0.8\times10^{-9}\,\mathrm{s}$. The inset in Fig. 1 illustrates that two distinct power-law regions are observed only for curves 5–7 when traps are not saturated. However, the main plot in Fig. 1 shows $\Delta n(t)$ begins to bend at longer times, deviating from the ($t^{(-\alpha-1)}$) power-law. The effect of trap saturation is evident on curves 1–4. When all traps are saturated ($\Delta n_0 \gg N_\Sigma$) as for the curve 1, the initial fast exponential decay has a time constant of monomolecular recombination, τ_r. As Δn_0 decreases and trap occupation decreases, the time constant of the initial exponential decay begins to approach the average trapping time (curves 2–4). Eventually, for low trap occupation (curves 5–7) the time constant does not depend on Δn_0 values and is exactly equal to $\tau_{\downarrow av}$.

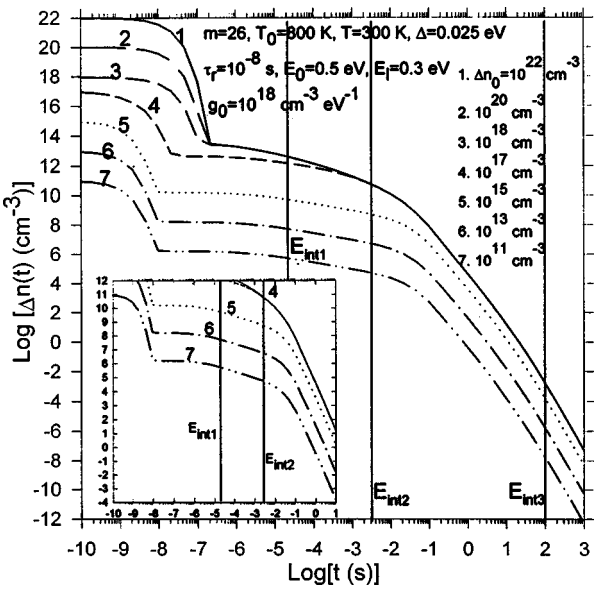

FIG. 1. Behavior of simulated transients of excess free electrons $[\Delta n(t)]$ for selected values of an initial excess electron concentration Δn_0 for condition (i) ($\tau_{\downarrow av}\cong 0.1\tau_r$). The inset: an enlarged part of the main plot covering the region having the two power-law components.

Because of the log/log plot the power law dependence would give a slope of $(\alpha-1)$ before the bend (knee) and $(-\alpha-1)$ after the knee. Under complete trap saturation, the slope is intensity independent before the knee and $\Delta n(t)$ is not linear in t (curve 1, Fig. 1). As time proceeds, electrons are released from levels; however, their retrapping is not uniform. Because deep traps are still saturated, electrons can be retrapped by shallower levels from which electrons have been thermally released. As Δn_0 is decreased, the slope (curves 3 and 4 on Fig. 1) starts to respond to Δn_0 changes, but a linear behavior occurs only when saturation is removed completely, i.e., regions before and after the knee in $\Delta n(t)$ have different intensity dependencies. Then, the slope is independent of Δn_0 (curves 5–7 on Fig. 1).

To facilitate an interpretation of $\Delta n(t)$ kinetics we applied a time-energy diagram analysis[12,15] to predict power-law behavior. The main idea of the diagram is to plot an individual trapping time $\tau_{\downarrow i}\equiv 1/\omega_i=1/(SvN_i)$, an individual release time $\tau_{\uparrow i}\equiv 1/r_i=1/v_0\exp(\delta E_i/kT)$ and the recombination time for each ith level in the distribution. Figure 2 shows this plot for three values of g_0. Intersections between the corresponding lines indicate energy associated with $\Delta n(t)$ at some time interval. First, consider the two intersections between the horizontal recombination time line and the individual trapping time curve for $g_0=10^{18}\,\mathrm{cm}^{-3}\,\mathrm{eV}^{-1}$. These correspond to two energies, $E_{\mathrm{int}\,1}$ and $E_{\mathrm{int}\,2}$. The electron release times from these two levels to the conduction band are shown on Fig. 1 as vertical lines. The region between these lines displays the $(\alpha-1)$ power-law behavior (curves 5–7). Thus, for the Gaussian DOS the condition for this power law region is $\tau_{\downarrow i}<\tau_r,\tau_{\uparrow i}$, which corresponds to subsequent carrier retrapping in states located between energy levels $E_{\mathrm{int}\,1}$ and $E_{\mathrm{int}\,2}$, i.e., thermalization.

For energies greater than $E_{\mathrm{int}\,2}$, recombination dominates over thermal release and retrapping. In this case, there are

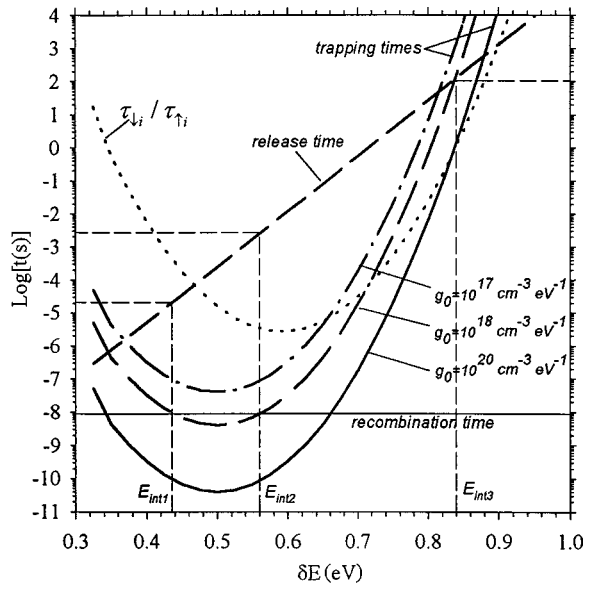

FIG. 2. The recombination time, the release time from individual traps, the individual trapping time and $\tau_{\downarrow i}/\tau_{\uparrow i}$ as a function of trap energy for selected values of g_0.

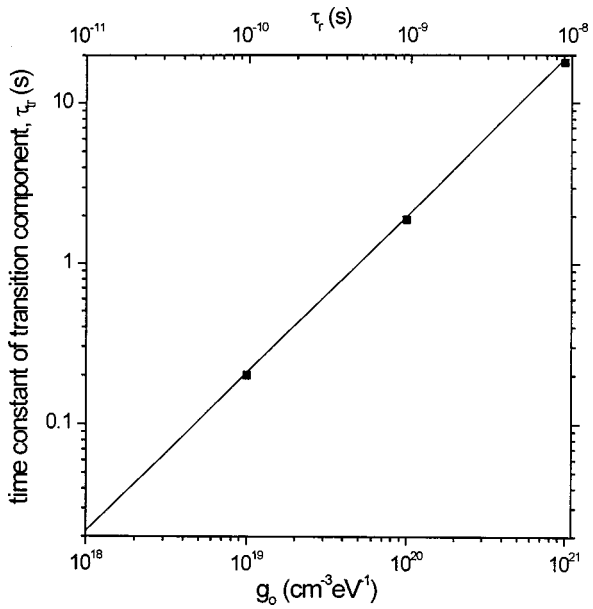

FIG. 4. The time constant of the transition exponential component as a function of g_0 and τ_r.

two subregions: $\tau_r < \tau_{\downarrow i} < \tau_{\uparrow i}$ and $\tau_r < \tau_{\uparrow i} < \tau_{\downarrow i}$, and the boundary between them is determined by the intersection between the individual trapping time curve and the release-time line (Fig. 2). This intersection occurs at energy $E_{\text{int}\,3}$ with its release time given in Fig. 1. Beyond this time, $\Delta n(t)$ deviates from a $(-\alpha-1)$ power-law behavior.

Condition (ii) is satisfied for g_0 ranging from $10^{21}\,\text{cm}^{-3}\,\text{eV}^{-1}$ to $10^{19}\,\text{cm}^{-3}\,\text{eV}^{-1}$. Typical behavior of $\Delta n(t)$ in this range is demonstrated in Fig. 3 for $g_0 = 10^{20}\,\text{cm}^{-3}\,\text{eV}^{-1}$ with seven curves corresponding to different values of Δn_0 ($10^{22} - 10^{11}\,\text{cm}^{-3}$). Analysis using the time-energy diagram is not straightforward because of complex kinetics. Trap saturation affects the initial exponential decay the same as condition (i).

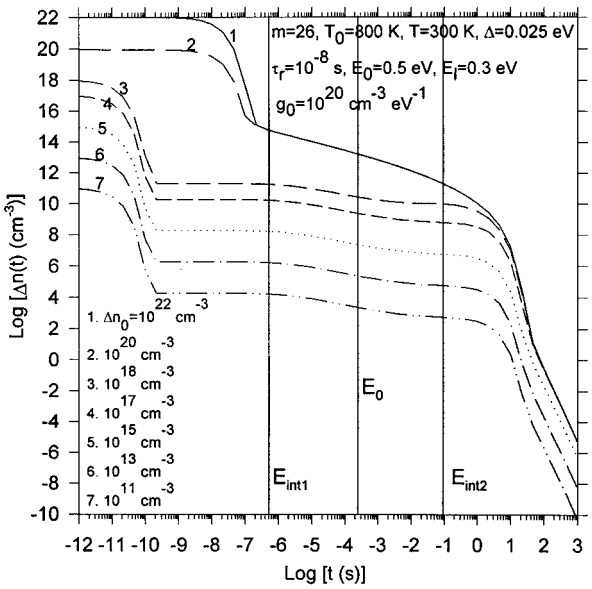

FIG. 3. Behavior of simulated transients of excess free electrons $[\Delta n(t)]$ for selected values of an initial excess electron concentration Δn_0 for condition (ii) ($\tau_{\downarrow av} < 0.1\tau_r$).

Following the initial exponential decay due to trapping (curves 3–7), a plateau region extends to approximately 5×10^{-7} s, corresponding to the release time (about 2×10^{-7} s) for the energy level $E_{\text{int}\,1}$ obtained at the first intersection point. Therefore, nothing happens until electrons from the shallowest level are released. The release time from the peak energy level E_0 appears somewhere between those designated by $E_{\text{int}\,1}$ and $E_{\text{int}\,2}$ in Fig. 3. A change in slope of $\Delta n(t)$ near the E_0 vertical line reflects the fact that the density of states increases with energy below E_0 and decreases above it. Although this region corresponds to thermalization, the behavior differs from the one for condition (i) where the slope remains the same below and above E_0. As the time is increased beyond $E_{\text{int}\,2}$ (Fig. 3) there is a ''transition'' exponential decay followed by a power-law decay for all transients. All seven curves gave the same fit of the exponential region over five orders of magnitude with a time constant $\tau_{tr} = 1.9$ s. The time constant depends linearly on g_0 and τ_r values (Fig. 4). This graph shows two plots: the first, τ_{tr} vs g_0 for three g_0 values and $\tau_r = 10^{-8}$ s; and the second, τ_{tr} vs τ_r for three τ_r values and $g_0 = 10^{21}\,\text{cm}^{-3}\,\text{eV}^{-1}$. The two plots indicate that an increase by one order of magnitude in g_0 can be compensated by an increase by one order of magnitude in τ_r.

It seems possible that the exponential decay is dominated by one energy level. To determine this level we use $\tau_{tr} = \tau_r \tau_{\uparrow i}/\tau_{\downarrow E_0}$, which is analogous to an expression derived in Ref. 10 for strong re-trapping. The time of trapping to level E_0, $\tau_{\downarrow E_0}$, is used because it has the maximum density and will be the dominant trap. With this equation and the parameters in Fig. 4, it turns out that all three points give the same ith energy level ($\sim$0.59 eV). Since the energy level that satisfies $\tau_{tr} = \tau_r \tau_{\uparrow i}/\tau_{\downarrow E_0}$ must be ''maximally'' filled with electrons most of the time, this value should occur at the minimum in the ratio $\tau_{\downarrow i}/\tau_{\uparrow i}$ vs the energy of the trap. (Indeed, the level should be not only effective in trapping but also in keeping electrons). From a plot of $\tau_{\downarrow i}/\tau_{\uparrow i}$ vs energy (Fig. 2),

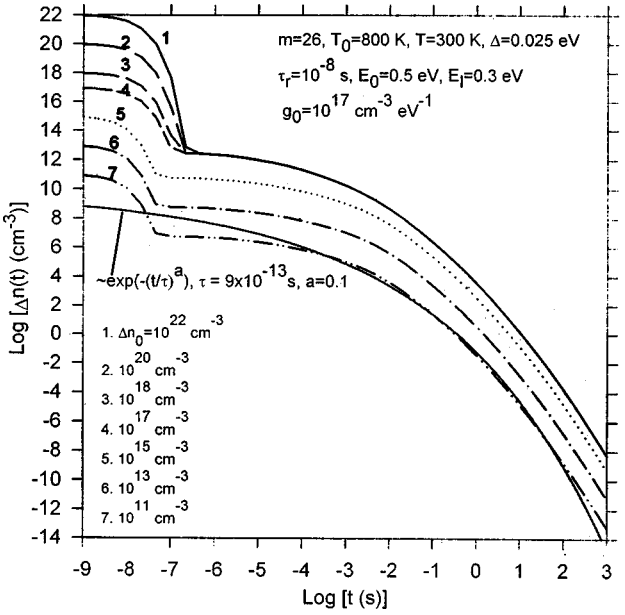

FIG. 5. Behavior of simulated transients of excess free electrons $[\Delta n(t)]$ for selected values of an initial excess electron concentration Δn_0 for condition (iii) ($\tau_{\downarrow av} > 0.1\tau_r$).

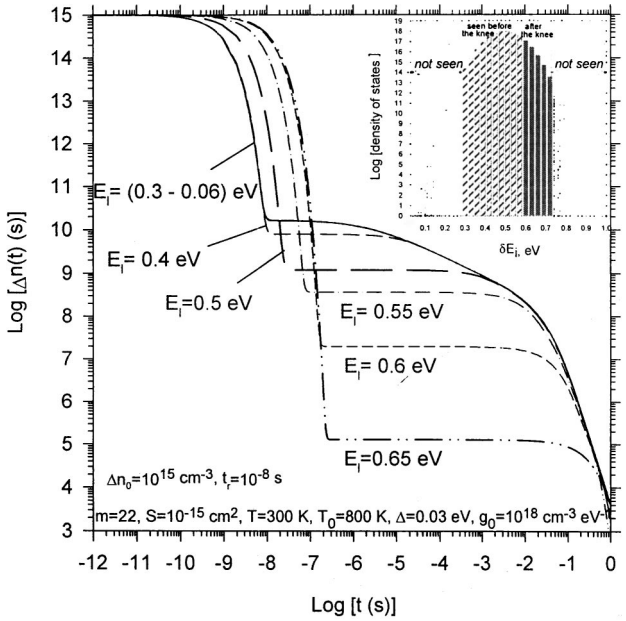

FIG. 6. Behavior of simulated transients of excess free electrons $[\Delta n(t)]$ for selected values of the offset energy E_1 for condition (i) ($\tau_{\downarrow av} \cong 0.1\tau_r$). The inset: the total Gaussian distribution used for the simulation.

this minimum is calculated to occur at 0.59 eV. Therefore, the exponential decay is due to thermal release from a level other than E_0 for condition (ii).

Condition (iii) was analyzed for g_0 ranging from $10^{14}\,\mathrm{cm^{-3}\,eV^{-1}}$ to $10^{17}\,\mathrm{cm^{-3}\,eV^{-1}}$. Typical behavior of $\Delta n(t)$ is shown in Fig. 5 for $g_0 = 10^{17}\,\mathrm{cm^{-3}\,eV^{-1}}$, which demonstrates no power law (no linear regions) for all Δn_0 values. Although a single analytical expression could not describe the total decay, the region from 10^{-4} to 10^{2} s corresponding to about 15 orders of magnitude in $\Delta n(t)$ can be fit by a stretched-exponential decay (Williams-Watts function). Originally, this function was derived for a model involving recombination on mobile defects.[16] However, it can no longer be considered diagnostic for this model because Fig. 5 demonstrates that trapping at stationary defects with a Gaussian DOS under condition (iii) can provide the same function. These three conditions with similar transients can also be obtained when g_0 is constant and τ_r is varied.

Finally, for the distribution satisfying condition (i) we found that $\tau_{\downarrow 0.59} \cong \tau_r$. Because the importance of this level is now clear criteria (ii) and (iii) can be rewritten in terms of $\tau_{\downarrow 0.59}$ as $\tau_{\downarrow 0.59} < \tau_r$ and $\tau_{\downarrow 0.59} > \tau_r$, correspondingly. Applying this knowledge to Fig. 2, one see that the point corresponding to $\tau_{\downarrow 0.59}$ on the trapping time curve for $g_0 = 10^{18}\,\mathrm{cm^{-3}\,eV^{-1}}$ [condition (i)] is indeed close to the horizontal recombination time line. At this unique condition only the intersection points $E_{\mathrm{int}\,1}$ and $E_{\mathrm{int}\,2}$ give the region of the first power-law decay corresponding to thermalization. For the curve with $g_0 = 10^{20}\,\mathrm{cm^{-3}\,eV^{-1}}$ [condition (ii)] there are still two intersection points ($E_{\mathrm{int}\,1}$,$E_{\mathrm{int}\,2}$), however, the point corresponding to $\tau_{\downarrow 0.59}$ on the trapping time curve is located well below the recombination time line, and no power-law in a thermalization region is observed. For the condition (iii) ($g_0 = 10^{17}\,\mathrm{cm^{-3}\,eV^{-1}}$) the point $\tau_{\downarrow 0.59}$ is located well above the recombination time line, and no power law is observed as well.

2. Effect of regions of the distribution on power-law behavior

For simplicity, we consider the decay for condition (i) when both power-law components are resolved. For this analysis the Gaussian distribution is kept fixed with the peak energy $E_0 = 0.5$ eV. The contribution of particular regions of the Gaussian distribution to either the $(\alpha - 1)$ or $(-\alpha - 1)$ regions could be ascertained varying the offset value, E_l from 0.06 to 0.65 eV while the energy range was held constant (22 levels with an energy step of 0.03 eV). Thus, an offset value of 0.06 eV provided an energy range between 0.06 and 0.73 eV for numerical calculation of $\Delta n(t)$. All numerical solutions were obtained for non-saturation ($\Delta n_0 = 10^{15}\,\mathrm{cm^{-3}}$ and $g_0 = 10^{18}\,\mathrm{cm^{-3}\,eV^{-1}}$ with other parameters given above). The maximum time was limited to 1 s, the release time from 0.73 eV level, which firmly set the upper boundary for the level that could be accessed. The transient remained virtually unchanged when E_l was changed from 0.06 to 0.3 eV (Fig. 6), indicating these levels remained invisible in the simulated data. This transient consisted of an initial fast exponential decay followed by a small plateau region and subsequently by the two power-law decays. For these offsets the time constant of the exponential component remained the same, indicating that the rate of the initial removal of electrons from the conduction band was unchanged. An exponential fit of this decay gave a time constant of 7.6×10^{-10} s and a pre-exponential factor of 10^{15}, which is identical to the initial excess electron concentration used in the numerical solutions. Furthermore, this time constant is very close to the average trapping time $[\tau_{\downarrow av} = 1/(S v \Sigma_{i=1}^{22} N_i)]$ of 8×10^{-10} s, indicating the fast exponential decay corresponds to initial trapping.

The value of E_l affects the total concentration of states available for trapping. The inset in Fig. 6 depicts this effect. As mentioned above, states from 0.3 to 0.73 eV (shaded area) are visible in the numerical solution, and the total area

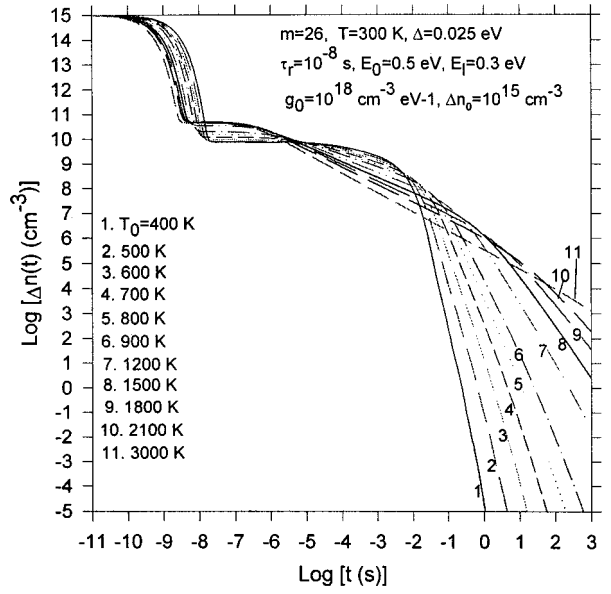

FIG. 7. Behavior of simulated transients of excess free electrons $[\Delta n(t)]$ for selected values of the characteristic temperature (T_0) of the distribution.

between these two values determines the trapping time constant. This conclusion is apparent because the exponential time constant was unchanged when the levels between 0.06 and 0.3 eV were removed by increasing E_l in this range. The reason is the much lower the density of these levels in comparison to those above 0.3 eV. For the same reason, levels deeper than 0.73 eV do not affect the transient for time below 1 s.

Because $d\Delta n(t)/dt=0$ in the plateau region, the rate of release from the traps must be equal the recombination rate plus the trapping rate. This condition breaks down at a time corresponding to release from the 0.3 eV level and is approximately the point where the first power-law decay starts. Between $E_l=0.3$ and 0.5 eV the plateau region increases at the expense of the $(\alpha-1)$ power law region. As one can see it affected only the middle part of the kinetics by extending the plateau region to longer times. However, the time constant of the initial exponential decay was the same, indicating that the density of the levels removed from the distribution was not high enough to affect the trapping rate. Above $E_l=E_0=0.5\,\mathrm{eV}$, the time constant of the fast exponential decay starts to increase, indicating levels of appreciable density are removed to slow down the trapping process. It should be mentioned that levels deeper than 0.73 eV are added and shallower levels are removed as E_l is increased because the numerical calculation always uses 22 energy steps. However, the increase in time constant indicates the added density of the levels deeper than 0.73 eV is too low to affect the trapping rate.

When $E_l=0.55\,\mathrm{eV}$, the plateau extends to the beginning of the knee position. Subsequent increase in the offset from 0.55 to 0.6 eV has two effects: freezing the time constant of the fast exponential decay and extending the plateau into the second power-law part in $\Delta n(t)$. Fitting this fast decay now gives 10^{-8} s as a time constant which is the same as the recombination time. Since the fast exponential decay always corresponds to the fastest process, it is understandable that the time constant will correspond to the trapping rate when the trap density is high and to the recombination rate at about $E_l=0.6\,\mathrm{eV}$ when the density is low. Beyond this point, the time constant is not affected by changes in the total density of centers. One can see from Fig. 6 that a transition from one power-law decay to the other occurs for an energy level located between 0.55 and 0.6 eV, not at the peak energy $E_0=0.5\,\mathrm{eV}$. This result is consistent with the conclusion made in a previous section that the knee is located at a time close to the release time of the most effective trap in the Gaussian DOS, i.e., 0.59 eV in this case. In Fig. 6, the total shaded area in the distribution indicates the levels effective for the numerical solution of the decay. The light gray area affects the decay before the knee, and the dark gray area affects the region after the knee.

3. Effect of the width of the gaussian distribution on power-law decays

Monte Carlo simulations[8,17] of time-of-flight photocurrents showed that this distribution can produce a transition from one power law $(t^{1-\alpha})$ to the other $(t^{-1-\alpha})$. Furthermore, the two power laws did not give the same α value, and the temperature dependence did not always follow $\alpha \propto T/T_0$. In this section, the behavior of α is explored with our multiple trapping model, i.e., using recombination rather than diffusion term. Numerical calculations were made for unsaturated traps: $g_0=10^{18}\,\mathrm{cm^{-3}\,eV^{-1}}$, $\tau_r=10^{-8}$ s, $\Delta n_0=10^{15}\,\mathrm{cm^{-3}}$, $T=300\,\mathrm{K}$ with other parameters same as

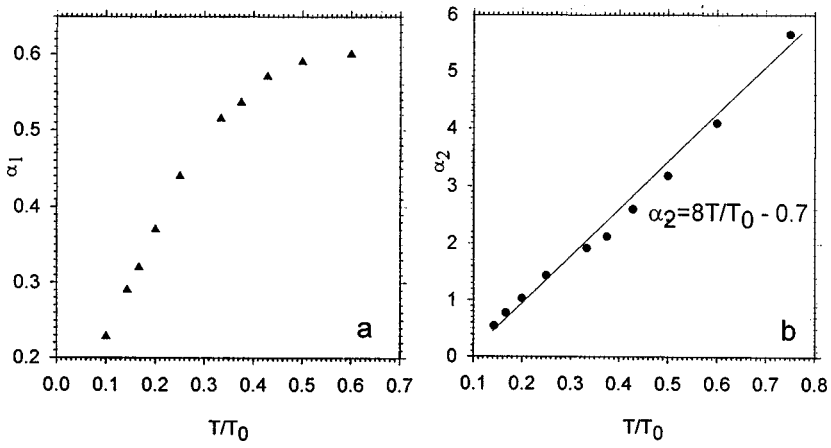

FIG. 8. Exponents of the power-law decay extracted from the region before the knee, α_1 (a) and after the knee, α_2 (b) as functions of T/T_0 for condition (i) $(\tau_{\downarrow av}\cong 0.1\tau_r)$.

TABLE I. Values of the first and last levels detectable by experiment at selected temperatures for the distribution discussed in the text.

T, K	kT, eV	E_{t1}, E_V	E_{t2}, eV	$E_{t2}-E_{t1}$, eV
123	0.0106	0.122	0.244	0.122
203	0.0175	0.201	0.402	0.201
300	0.0258	0.297	0.594	0.297
358	0.0308	0.354	0.709	0.354

above. The curves for various T_0 in Fig. 7 demonstrate the width of the distribution affects the slopes before and after the knee. Furthermore, the first power law shrinks as T_0 decreases. Values of α_1 (before the knee) and α_2 (after the knee) obtained by fits show that $\alpha_1 \neq \alpha_2$ [Figs. 8(a) and 8(b)]. While α_2 shows a linear temperature dependence over the whole range of T/T_0, the linear range for α_1 is limited. Compared to the Monte Carlo simulations done in the $T/T_0 = 0.1-0.5$ range,[8] our α_1 values are somewhat lower for $T/T_0 \geqslant 0.5$ (≈ 0.6 compared to ≈ 0.8 at $T/T_0 = 0.5$). Our results indicate that values >0.6 are difficult to obtain for the Gaussian DOS. Indeed, as T approaches T_0 (or vise versa) the $t^{1-\alpha}$ region shrinks and eventually is not obtained. Since our calculations were done over a larger dynamic range of $\Delta n(t)$, our α values probably are more reliable. Unless a large range is used, the extraction of the true power-law exponent can be obscured by the proximity of the knee region. Finally, the time range where power-law decays exist is limited in Fig. 7. However, this limitation is due to the value of E_0 chosen; a larger value moves the transient to longer times without affecting α.

4. Detecting the Gaussian distribution in experiments

If measurements are made over a given time range only a limited part of the real distribution is probed at a particular temperature. For example, consider an experiment in which the time is $10^{-7}-10^{-2}$ s and measurements are done at four selected temperatures (123, 203, 300, 358 K). Only the levels with release times falling within the time range will affect the kinetics at each temperature. Calculations of the first (E_{t1}), the last (E_{t2}) levels detected and the effective width probed ($E_{t2}-E_{t1}$) are summarized in a Table I. Increasing the temperature enlarges the width and moves the trap levels deeper.

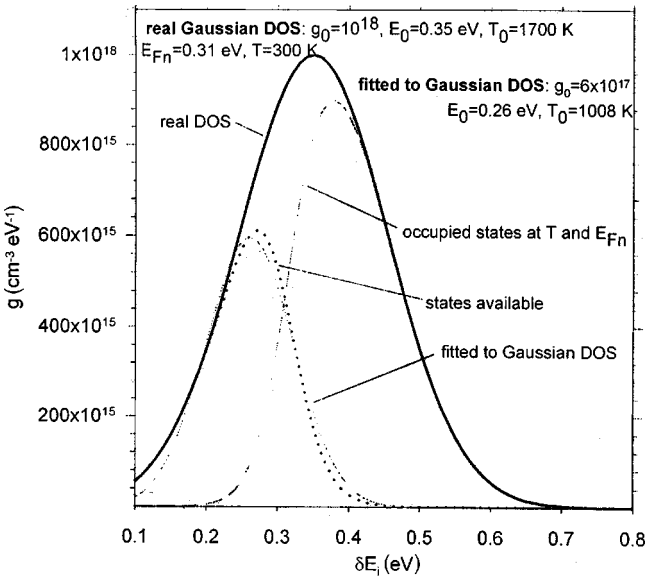

FIG. 9. The real Gaussian DOS, occupied states determined by the Fermi function, states available and fitted to Gaussian DOS ($T = 300$ K).

Accordingly, it would seem possible to map out the complete distribution by a series of measurements at various temperatures; however, this approach cannot work because the range of energy levels that are occupied in the dark at equilibrium is temperature dependent. The ramifications of this dependence can be seen by analyzing the occupation level of any Gaussian DOS $[g(E)]$ in the band gap (for example: $g_0 = 10^{18}\,\mathrm{cm}^{-3}\,\mathrm{eV}^{-1}$, $T_0 = 1700\,\mathrm{K}$, $E_0 = 0.35\,\mathrm{eV}$). At any temperature, only part of this DOS will be available for multiple trapping processes because some states will be occupied at equilibrium before illumination. The density of the levels $[g_{oc}(E)]$ occupied at equilibrium is a product of the density of localized states $[g(E)]$ and the Fermi function $f(E)$:

$$g_{oc}(E) = g_0 \exp\{-[(E-E_0)/kT]^2\} f(E) \tag{3}$$

in which $f(E) = 1/[\exp(-E+E_{Fn})/kT+1]$ is the occupation probability. The density of states $[g_{av}(E)]$ available for trapping electrons is,

$$g_{av}(E) = g(E) - g_{oc}(E). \tag{4}$$

For calculations, $T = 300\,\mathrm{K}$ and $E_{Fn} = 0.31\,\mathrm{eV}$, which was taken as the equilibrium electron Fermi level position at 300 K. Comparison of curves $[g(E),\ g_{oc}(E),\ g_{av}(E)]$ in Fig. 9 indicates that the density of available states involves only a small portion of the total DOS. Furthermore it does not have Gaussian shape, as indicated by the attempted fit of $g_{av}(E)$ to a Gaussian DOS shown in Fig. 9. As expected, the fit parameters ($g_0 = 6\times10^{17}\,\mathrm{cm}^{-3}\,\mathrm{eV}^{-1}$, $T_0 = 1008\,\mathrm{K}$, $E_0 = 0.26\,\mathrm{eV}$) are far away from those for the real DOS. The shape of $g_{av}(E)$ suggests that the left (low-energy) side continues to follow the low-energy side of $g(E)$ while the right (high-energy) part is truncated smoothly and distorted from the Gaussian DOS by occupied states at the specific T and E_{fn}. (Note, that one may observe trapping and thermal release for levels located *below* the Fermi level).

The effect of a decrease in temperature depends on the direction in which the Fermi level moves. For the same Gaussian DOS used at 300 K, the available levels were calculated at 123 K assuming the electron Fermi level moved closer to the conduction band to the position $E_{Fn} = 0.21\,\mathrm{eV}$. Since either direction is possible depending on the material,[18] this direction was chosen for illustration purposes only. As might be expected, the plots of $g(E)$, $g_{oc}(E)$, $g_{av}(E)$ and the fitted curve in Fig. 10 indicate the curve corresponding to the density of available states narrowed and moved to lower energies. These results clearly indicate that transients at a particular temperature can provide evidence only for an *effective* density of states that deviates markedly from the actual DOS. Furthermore, combining DOS obtained at various temperatures will not completely reproduce the

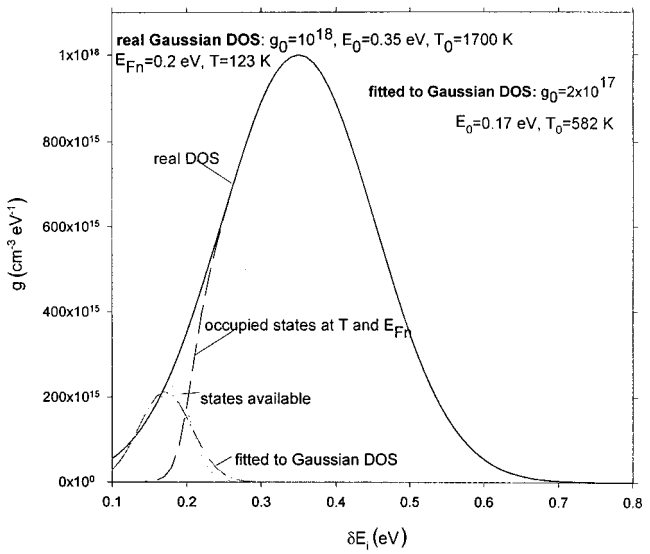

FIG. 10. The real Gaussian DOS, occupied states determined by the Fermi function, states available and fitted to Gaussian DOS ($T=123$ K).

actual Gaussian DOS of the semiconductor unless the effective distribution is deconvoluted with the Fermi function.

Turning now to the temperature dependence of α, some authors observed experimentally that α either decreased or remained constant with increasing temperature.[1] For most (if not for all) types of DOS assuming the validity of multiple trapping, this observation contradicted the expected increase of α with increased temperature according to the relation $\alpha \propto T/T_0$. Obviously, this relation cannot account for the observed decrease of α with increased temperature. To explain this behavior some authors[1] suggested a model in which an increase in temperature transforms traps into recombination centers with different capture crosssections for electrons and holes.

Our results presented above, provide another explanation. Because the width of the available or effective DOS increases with increased temperature, the temperature behavior of α has the form $\alpha \propto (T+\Delta T)/(T_0+\Delta T_0)$ in which ΔT_0 is associated with the width of the effective DOS. When ΔT_0 is bigger than ΔT, α decreases with increasing temperature. As demonstrated above, the width of the effective DOS is small at low temperatures and increases at higher temperatures until the Fermi level moves down towards the middle of the band gap. Above this temperature, the width of the effective DOS will not change much because it corresponds closely to the one for the real DOS. As a result, the negative changes in α are expected at temperatures where ΔT_0 is largest. The exact temperature range where this occurs will depend on the temperature dependence of the Fermi level.

For an exponential DOS, α is expected to follow the relation $\alpha \propto T/T_0$ more closely because the shallower energy levels have the highest densities. As a result, movement of $f(E)$ toward midgap would cause less severe effects.

IV. CONCLUSIONS

A Gaussian DOS of subband gap states has been used to analyzed the transient behavior of excess carriers within a multiple-trapping model with a recombination term rather than a diffusion term. For this DOS, the behavior of $\Delta n(t)$ varies according to three conditions relating trapping time of the optimally filled energy level to recombination time. It was demonstrated that this DOS provides the two power-law regions only under very limited conditions. Under these conditions, the knee between the two power laws occurs at a time corresponding to the thermal release of electrons from the optimally filled energy level for which $\tau_{\downarrow i}/\tau_{\uparrow i}$ has a minimum. Levels having energies lower than this optimum control the power-law decay before the knee, and those above are responsible for the power-law decay after the knee. The exponents of the two power laws, α_1 and α_2 are related to the width of the distribution. The maximum value of α_1 cannot exceed 0.6 for the Gaussian DOS. Finally, we showed that at some conditions the experimental transients may provide only an effective distribution of localized states which does not coincide with the real Gaussian DOS present in the sample. The parameters of this effective DOS depend on temperature, which controls the position of the dark Fermi level. The effective DOS is distorted from the Gaussian form by the Fermi occupation function. The variation in a width of the effective DOS may explain the experimentally observed decrease of α_1 with increased temperature.

ACKNOWLEDGMENT

This work was supported in part by a grant from the Natural Sciences and Engineering Research Council to M.C.

*Present address: Department of Physics, 60 St. George St., University of Toronto, Toronto, Ontario M5S 1A7 Canada.

[1] G. J. Adriaenssens and P. Nagels, J. Non-Cryst. Solids **114**, 100 (1989).

[2] C. Main, in *Transient Phenomena*, edited by M. Schwarz, MRS Symposia Proceeding No. 467 (Materials Research Society, Pittsburgh, 1997), p. 167.

[3] H. Naito, T. Nagase, T. Ishii, M. Okuda, T. Kawaguchi, and S. Maruno, J. Non-Cryst. Solids **198-200**, 363 (1996).

[4] J. Orenstein, M. A. Kastner, and V. Vaninov, Philos. Mag. B **46**, 23 (1982).

[5] J. Tauc, in *Semiconductors and Semimetals*, edited by J. I. Pankove (Academic, Orlando, 1984), Vol. 21 B, Chap. 9.

[6] P. Grygel and W. Tomaszewicz, J. Phys.: Condens. Matter **9**, 10 381 (1997).

[7] S. Grabtchak and M. Cocivera, Phys. Rev. B **50**, 18 219 (1994); Prog. Surf. Sci. **50**, 305 (1995); J. Appl. Phys. **79**, 786 (1996); Phys. Rev. B **58**, 4701 (1998).

[8] J. M. Marshall, H. Michiel, and G. J. Adriaenssens, Philos. Mag. B **47**, 211 (1983).

[9] B. Hartenstein, H. Bässler, A. Jakobs, and K. W. Kehr, Phys. Rev. B **54**, 8574 (1996).

[10] S. Grabtchak and M. Cocivera, Philos. Mag. B **77**, 49 (1999).

[11] S. Grabtchak and M. Cocivera, Phys. Rev. B **58**, 12 594 (1998).

[12] S. Grabtchak and M. Cocivera, Philos. Mag. B **79**, 881 (1999).

[13] A. J. Campbell, D. D. C. Bradley, and D. G. Lidzey, J. Appl.

Phys. **82**, 6326 (1997).
[14] H. Bassler, Intern. J. Mod. Phys. **8**, 847 (1994).
[15] S. Grabtchak, Ph.D. thesis, University of Guelph, 1998.
[16] M. F. Shlesinger and E. W. Montroll, Proc. Natl. Acad. Sci. USA **81**, 1280 (1984).
[17] J. M. Marshall, Philos. Mag. **36**, 959 (1977).
[18] M. Alibzhonov, M. A. Karimov, M. S. Saidov, and N. Kh. Yuldashev, Semiconductors **30**, 827 (1996).